ACS OMEGA

Open Access

http://pubs.acs.org/journal/acsodf

Article

Fibrin-Polycaprolactone Scaffolds for the Differentiation of Human Neural Progenitor Cells into Dopaminergic Neurons

Salma P. Ramirez, Ivana Hernandez, Zayra N. Dorado, Carla D. Loyola, David A. Roberson, and Binata Joddar*

Cite This: *ACS Omega* 2024, 9, 37063−37075

Read Online

ACCESS | Metrics & More | Article Recommendations | Supporting Information

ABSTRACT: Parkinson's disease (PD), a progressive central nervous system disorder marked by involuntary movements, poses a significant challenge in neurodegenerative research due to the gradual degeneration of dopaminergic (DA) neurons. Early diagnosis and understanding of PD's pathogenesis could slow disease progression and improve patient management. In vitro modeling with DA neurons derived from human-induced pluripotent stem cell-derived neural progenitor cells (NPCs) offers a promising approach. These neurons can be cultured on electrospun (ES) nanofibrous polycaprolactone (PCL) scaffolds, but PCL's hydrophobic nature limits cell adhesion. We investigated the ability of ES PCL scaffolds coated with hydrophilic extracellular matrix-based biomaterials, including cell basement membrane proteins, Matrigel, and Fibrin, to enhance NPC differentiation into DA neurons. We hypothesized that fibrin-coated scaffolds would maximize differentiation based on fibrin's known benefits in neuronal tissue engineering. The scaffolds both coated and uncoated were characterized using scanning electron microscopy (SEM), transmission electron microscopy, Fourier transform infrared spectroscopy-attenuated total reflectance, and dynamic mechanical analysis to assess their properties. NPCs were seeded on the coated scaffolds, differentiated, and matured into DA neurons. Immunocytochemistry targeting tyrosine hydroxylase (TH) and SEM confirmed DA neuronal differentiation and morphological changes. Electrophysiology via microelectrode array recorded their neuronal firing. Results showed enhanced neurite extension, increased TH expression, and active electrical activity in cells on fibrin-coated scaffolds. Diluted fibrin coatings particularly promoted more pronounced neuronal differentiation and maturation. This study introduces a novel tissue-on-a-chip platform for neurodegenerative disease research using DA neurons.

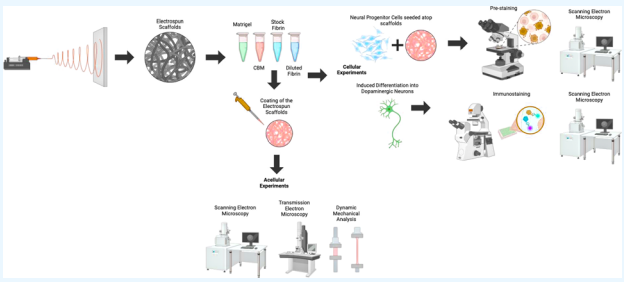

1. INTRODUCTION

Parkinson's Disease (PD) is a neurological disorder affecting involuntary movements that progressively worsen. PD poses a significant challenge in neurodegenerative research due to its progressive nature and the profound impact it has on patients' lives. A significant factor in the progression of this disease is the deterioration of dopaminergic (DA) neurons within the central nervous system (CNS).[1] Annually, around 90,000 individuals are diagnosed with PD in the United States,[2] a figure that is rising from previous estimates. It is estimated that by 2030, approximately 1.2 million people in the United States will suffer from this disease.[3] Thus, it is crucial to conduct more research to track the early onset and progression of PD for designing effective treatment strategies. Understanding the early stages and underlying mechanisms of PD could potentially provide pathways for slowing disease progression and enhancing patient care, especially considering the crucial importance of early diagnosis.

A promising approach for investigating the initial stages and developmental pathogenesis of PD involves the use of in vitro tissue models, consisting of appropriate cellular components and scaffolds. An optimal scaffold should possess sites for cell attachment along with signals to stimulate cellular differentiation.[4]

The addition of human-induced pluripotent stem cell (hiPSC)-derived neuronal progenitor cells (NPCs) offers a platform for studying neurodegenerative disease mechanisms such as those involved in the progression of PD. In this study, we used NPCs, since they undergo similar cellular division processes as those in the human CNS,[5,6] leading to the formation of embryonic layers and organ-specific tissues. Using NPCs allows the modeling of early neurodevelopment accurately, providing a relevant system for studying the differentiation and maturation of DA neurons, which are crucial for understanding PD.

Received: April 24, 2024
Revised: June 21, 2024
Accepted: June 27, 2024
Published: August 21, 2024

The overall goal of this research was to implement electrospun (ES) polycaprolactone (PCL) scaffolds with various extracellular matrix-based (ECM)-based coatings to promote NPC cell adhesion and DA neuronal differentiation. Cultivating these cells on ES nanofibrous PCL scaffolds provides an environment that mimics the architecture of the native ECM, which promotes cell adhesion and their differentiation into DA neurons.[7] However, challenges arise with PCL scaffolds as they are not only hydrophobic but also lack the functional biological groups critically needed for cell adhesion and differentiation, presenting challenges for their use and adoption as scaffolds. To address this, we investigated the effectiveness of coating the ES PCL scaffolds with hydrophilic ECM-based biomaterials, such as Cell Basement Membrane (CBM), Matrigel, and Fibrin (in varying concentrations).

CBM is a complex mixture of proteins and glycoproteins found in the ECM of various tissues.[8] Derived from murine Engelbreth-Hol-Swarm (EHS) tumor, CBM stands as a highly recommended substrate for culturing induced pluripotent stem cells (iPSCs) due to its ability to provide both structural support and biochemical cues that influence cell behavior, including cell adhesion, migration, and differentiation.[9] Coating hydrophobic ES PCL scaffolds with CBM can mimic the natural microenvironment of NPCs, promoting their attachment and guiding their differentiation into specific cell types, such as DA neurons. Likewise, Matrigel is a widely available ECM extract derived from mouse sarcoma cells. It contains a rich mixture of ECM proteins, growth factors, and other signaling molecules that support cell adhesion, proliferation, and differentiation.[10] Moreover, fibrin, a fibrous protein that plays a crucial role in blood clotting and wound healing,[10,11] emerges as a compelling choice in tissue engineering applications. Notably, fibrin can be used as a biocompatible and biodegradable substrate, offering a range of reported advantages, particularly in stem cell growth and differentiation. Because the fibrin network, upon polymerization, incorporates various adhesive proteins such as fibronectin (FN) and laminin (La), which are fundamental in transmitting cues for cell proliferation, viability, and differentiation,[4,12,13] it was selected to promote the adhesion and proliferation of NPCs and induce their differentiation into DA neurons.

For this study, acellular characterization of the scaffolds was performed by using Scanning Electron Microscopy (SEM), Transmission Electron Microscopy (TEM) for gross morphological comparisons, Fourier Transform Infrared Spectroscopy (ATR-FTIR) for chemical identification, and Dynamic Mechanical Analysis (DMA) for mechanical characterization.

Subsequently, NPCs were seeded onto the scaffolds, differentiated, and allowed to mature into DA neurons. Precell staining was performed using a cell membrane marker, PKH67, to observe the length of cellular extensions before inducing the differentiation into DA neurons as well as cell adhesion to the ES PCL scaffolds, alongside SEM to analyze cell morphology before the differentiation process. Immunocytochemistry targeting tyrosine hydroxylase (TH) expression was performed to validate DA differentiation, as well as SEM, which was performed to analyze the morphological changes of cells after differentiation. Lastly, electrophysiology via a microelectrode array (MEA) technique was employed to validate and confirm DA neuronal differentiation.

2. MATERIALS AND METHODS

2.1. Electrospinning of PCL Scaffolds. The equipment utilized to produce the PCL fibers was developed in-house, based on our previous published work;[14] the electrospinning setup can be observed in Supporting Information Figure S1. A 0.05% w/v PCL polymer solution was prepared by weighting 1.425 g of PCL and dissolving it in 25.20 mL of Hexafluoroisopropanol (HFIP) (0.25:3 ratio) as reported by our group previously.[15] The dissolved solution was mixed with a magnetic stirrer for 6−8 h until a homogeneous mixture was obtained. It was then loaded in 10 mL syringes with a 22 G needle connected to the positive terminal of a high-voltage DC supply (ES30P 10 W power supply, Gamma High Voltage Research, Ormond Beach, FL). Fibers were electrospun at room temperature (26 °C) and a relative humidity of 72%, with a current of 0.03 mA and a voltage of 18 kV, for 15−30 min per deposition. The fibers generated were collected onto a grounded aluminum rotating collector positioned 15 cm away perpendicular to the needle. Following electrospinning, the scaffolds were rinsed with 1X PBS, air-dried overnight, and stored at room temperature. The resulting samples were then sectioned into circular pieces measuring 19.1 mm in diameter and sterilized with UV light for 20 min.

2.2. Coating Solutions Preparation. *2.2.1. Cell Basement Membrane (CBM).* Cell Basement Membrane (CBM) is purified from murine EHS tumor and is a vendor-recommended ECM material for culturing iPSCs-derived NPCs.[16] The CBM used in this study is actually the vendor's recommended substrate for culturing NPCs and their targeted differentiation into DA neurons. The CBM (Cat. No. ACS-3035, ATCC, VA, USA) was thawed at 4 °C overnight following the vendor's instructions. 43 μL of the CBM solution with an initial concentration of 14 mg/mL was added to 4 mL of cold Dulbecco's Modified Eagle Medium F12 (DMEM: F12) (Cat. No. 30−2006, ATCC, VA, USA) growth medium to constitute a final concentration of 150 μg/mL. The solution was mixed thoroughly with a pipet. After complete dissolution, 500 μL of the coating solution was added to the PCL scaffolds, and samples were placed in a Belly Dancer Shaker for 10 min at 10 rpm. Thereafter, the coated scaffolds were incubated at 37 °C for at least 1 h under static conditions after which the coating solution was removed.

2.2.2. Matrigel. Published studies from others have reported the use of Matrigel, for the growth of NPCs.[10] It is a solubilized basement membrane preparation derived from the Engelbreth-Holm-Swarm (EHS) mouse sarcoma, a tumor rich in ECM, including Laminin and Collagen IV, and several growth factors, whereas CBM is purified from murine EHS tumor and contains factors specific to the basement membrane. Thus, Matrigel will influence neuron differentiation through its composition of ECM proteins and growth factors, whereas CBM contains factors specifically tailored to promote neural differentiation. Matrigel (Cat. No. 354234, Sigma-Aldrich, MO, USA) was thawed at 4 °C overnight following the vendor's instructions. Pipette tips used were kept cold at 4 °C along with DMEM: F12 growth medium (without FBS). After thawing, 50 μL of Matrigel was resuspended in 1 mL of DMEM: F12 growth medium. A pipet was utilized to mix the solution ensuring complete dissolution thoroughly. After preparing the coating solution, 19.1 mm circular PCL scaffolds were coated with 500 μL of the Matrigel-coating solution and placed in a Belly Dancer Shaker for 10 min at 10 rpm. The

https://doi.org/10.1021/acsomega.4c03952
ACS Omega 2024, 9, 37063−37075

coated scaffolds were then incubated at 37 °C for 1 h; after that time, the coating solution was removed.

2.2.3. Stock Fibrinogen. Fibrin-based scaffolds prepared using fibrinogen solution cross-linked using thrombin have been adopted by many studies to promote the growth and adhesion of NPCs and differentiate them toward CNS neurons.[12] Motivated by these findings our group also utilized fibrin-based scaffolds for maximizing the adhesion and differentiation of NPCs into DA neurons. To do this, Fibrinogen (20 mg/mL) coating was performed following the vendor's recommendations as described in previously published works.[17] Fibrinogen (Axolotl Biosciences, Canada) and the cross-linker solution containing thrombin and calcium chloride were thawed at 4 °C for 2 h. 500 μL of fibrinogen was added to each well in a 6-well plate atop the PCL scaffolds. Then, the plate was placed in a Belly Dancer shaker for 10 min at 10 rpm. 300 μL of the cross-linker solution was then added to each well and placed in the belly dancer shaker for 20 min at 10 rpm, and last, the cross-linker was removed.

2.2.4. Diluted Fibrinogen. Owing to the hydrophilicity of the underlying scaffold we hypothesized that diluting the stock or highly concentrated fibrinogen solution may be effective toward achieving a more widespread fibrin coating formation on the scaffolds. To do this, fibrinogen (Axolotl Biosciences, Canada) and the cross-linker containing thrombin and calcium chloride were thawed at 4 °C for 2 h. A diluted fibrinogen coating solution (10 mg/mL) was prepared following a protocol outlined in previously published work.[17] 250 μL of Fibrinogen and 250 μL of 1X PBS were mixed thoroughly to create the diluted fibrinogen solution with a final concentration of 10 mg/mL. 500 μL of the diluted fibrinogen coating solution was added to each well in a 6-well plate atop the PCL scaffolds. Then, the plate was placed in the Belly Dancer shaker for 10 min at 10 rpm. Thereafter, 300 μL of the cross-linker solution was added to each well and placed in the belly dancer shaker for 20 min at 10 rpm and then removed.

2.3. Cell Culture. The goal of this study was to implement electrospun PCL scaffolds coated with varying ECM biomaterials to support the growth and differentiation process of neural progenitor cells (NPCs) into dopaminergic neurons (DA). This cell type has been successfully utilized for DA differentiation in other published works,[18,19] in which NPCs have been used for the differentiation toward DA neurons. For this study, Neural Progenitor cells (ACS 5004, ATCC, VA, USA) were cultured according to the vendor's recommendations in a complete neural progenitor growth medium which consisted of the following components: 464 mL of Dulbecco's Modified Eagle Medium F12 (DMEM: F12) (Cat. No. 30−2006, ATCC, VA, USA) supplemented with the growth kit for neural progenitor cell expansion (Cat. No. ACS-3003, ATCC, VA, USA), 5 mL of L-Alanyl-L-Glutamine, 5 mL of Non-Essential Amino Acids, 10 mL of NPC Growth Kit Component A, 5 mL of NPC Growth Kit Component B, 1 mL of NPC Growth Kit Component C, and 10 mL of NPC Growth Kit Component D. A T-25 (ThermoFisher Scientific, Waltham, MA) flask was first coated with a cell basement membrane coating as described in section 2.2.1.; cells were then seeded at a cell density of 40,000 cells/cm^2 in the T-25 culture flask and cultured at 37 °C and 5% CO_2.

Cells were passaged when a 95% confluency was reached. For detaching and subculturing the cells, the complete growth medium was removed, and then undiluted accutase was added to the culture flask. The flask was incubated at 37 °C for 5−10 min until the majority of the cells were detached. After 10 min, DMEM: F12 was added in the same volume as the undiluted accutase to prevent cell damage. The cell-containing solution was then removed and transferred to a 15 mL conical tube. Cells were then centrifuged at 270 G for 5 min at room temperature. Thereafter, complete NPC growth media was added to resuspend the pellet. Cells were then seeded at a cell density of 70,000 cells/well in a 12-well culture plate containing previously coated ES PCL scaffolds. Before seeding, the scaffolds were examined under an optical microscope (EVOS XL Core, Zeiss, Germany) to confirm the presence of the coating. Cell adhesion and quantification on the scaffolds were confirmed using a routine cellular detachment procedure after 24 h with 0.25% Trypsin-EDTA (ThermoFisher) at 37 °C for 5 min (5% CO_2). The detached cells were pelleted following regular cell culture procedures and quantified using a Countess Automated Cell Counter (Invitrogen, Carlsbad, CA, USA).

2.3.1. Induced Differentiation toward a DA-Phenotype. Neural Progenitor Cells (ACS 5004, ATCC, Virginia, USA) were passaged and seeded at a cell density of 20,000 cells/cm^2 according to the vendor's recommendations in a T-25 flask (ThermoFisher Scientific, Waltham, MA). Dopaminergic neuronal differentiation was induced by culturing Neural Progenitor cells (Cat. No. ACS 5004, ATCC, VA, USA) in a STEMdiff Midbrain Neuron Differentiation Kit (Cat. No. 100−0038, STEM CELL Technologies) supplemented with Human Recombinant Shh (Cat. No. 78065, STEM CELL Technologies); medium change was performed daily for 14 days. Thereafter, the differentiation medium was replaced with STEMdiff Midbrain Maturation Medium (Cat. No.100−0041, STEM CELL Technologies) performing half medium change every 2−3 days for 13 days. The terminal point for the differentiation process was determined by daily optical microscope observations of cell morphology using an EVOS XL Core microscope (Zeiss, Germany).

2.4. Characterization of Uncoated and Coated ES PCL Scaffolds. Coated ES PCL scaffolds were freshly made a day before the experiments, kept at 4 °C to avoid the selective coating from degrading, and air-dried, prior to being subjected to other characterization analyses.

2.4.1. Scanning Electron Microscopy (SEM). SEM was performed to visualize the surface morphology of the uncoated electrospun scaffolds and their coatings, which included CBM, Matrigel, Stock Fibrin (20 mg/mL), and Diluted Fibrin (10 mg/mL). For doing SEM, samples were sputter-coated with gold/palladium for 3 min in a sputter coater (Gatan Model 682 Precision Etching Coating System Pleasantown, CA, USA) and were visualized using SEM (SU3500, Hitachi, Japan) at 10 kV voltage and current of 101.2 μA at varying magnifications.

2.4.2. Porosity. The SEM images acquired above were also adopted to measure the apparent porosity of the ES PCL scaffolds. Measurements were done using at least three images for each coating including CBM, Matrigel, Stock Fibrin (20 mg/mL), Diluted Fibrin (10 mg/mL), and uncoated scaffolds using ImageJ software according to published work;[20] however, the protocol was slightly modified to obtain accurate results for our scaffolds used in this study. The following process was followed for ImageJ calculations with all images: 1. The image was opened using the command "File > Open", 2. The image was thresholded to make the area of interest evident using the command "Image > Adjust > Threshold", 3. Analyzed particles were selected by using the command "Analyze > Analyze

https://doi.org/10.1021/acsomega.4c03952
ACS Omega 2024, 9, 37063−37075

Particles". From the resultant table, the area and % area occupied by the porosity in the scaffolds were obtained. The percentage (%) porosity of all scaffolds, uncoated and coated, was reported in this study and calculated using the following formula:

$$\%\text{Porosity} = \frac{\text{Volume of Space Occupied by Porosity}}{\text{Total Volume}} \quad (1)$$

2.4.3. Transmission Electron Microscopy (TEM). TEM was conducted utilizing a JEOL NEOARM Low kV STEM (JEOL Solutions for Innovations, MA, USA) operated with an aberration-corrected setting and operating at an acceleration potential of 200 kV to analyze the coating homogeneity and thickness on the electrospun scaffolds with various coatings including CBM, Matrigel, Stock Fibrin (20 mg/mL), and Diluted Fibrin (10 mg/mL). ImageJ was used to perform a dimensional analysis of fiber and coating thickness. The following formula was used to determine coating thickness:

$$\text{Coating Thickness} = \text{Total Thickness (coated samples)} - \text{Fiber Thickness (uncoated samples)} \quad (2)$$

2.4.4. Attenuated Total Reflectance Fourier Transform Infrared Spectroscopy (ATR-FTIR). FTIR was performed on the acellular ES PCL scaffolds with various coatings (Matrigel, CBM, Stock Fibrin, and Diluted Fibrin) to confirm coating via probing their chemical composition and the underlying scaffolds. Measurements were performed on the electrospun scaffolds using a Thermo Mattison Spectrometer (Thermo-Mattison, MA, USA) equipped with a ZnSe ATR crystal. The spectrum of the samples was recorded from 400 to 4000 cm^{-1}.

2.4.5. Mechanical Testing. The mechanical properties of ES PCL scaffolds are crucial considerations in tissue engineering applications as they directly influence the scaffold's ability to support cell growth, proliferation, and tissue regeneration. To measure the mechanical properties of the acellular ES PCL scaffolds, dynamic mechanical analysis (DMA) was conducted utilizing a PerkinElmer DMA 8000 (PerkinElmer, Waltham, MA, USA) instrument in tension mode. The specimens were fabricated via the electrospinning method described earlier, using 20 mL of the PCL-HFIP solution to ensure samples with a thickness greater than 250 μm. Rectangular PCL samples with 9.71 mm in length, 0.36 mm in thickness, and 7.76 mm in width were maintained at room temperature during testing. Static stress and static strain were measured using a maximum load of 2N at a rate of 0.1 N/min and held at that condition for an additional 20 min. Elastic modulus was calculated using the following formula:

$$\text{Elastic modulus} = \text{Stress}/\text{Strain} \quad (3)$$

2.5. Detection of Cells, Undifferentiated and Differentiated DA Neurons. *2.5.1. Confocal Fluorescence Microscopy and SEM for Undifferentiated Cells.* To visualize cell adhesion on the ES PCL scaffolds as well as observe the length of cellular extensions before the differentiation process, Neural Progenitor cells were prestained with a green fluorescent cell membrane staining dye PKH67 (Cat. No. MINI67−1KT, Sigma-Aldrich, MO, USA). The prestaining of Neural Progenitor cells was performed as previously reported by our group[21] and following the vendor's instructions. Briefly, undiluted accutase was used to detach the cells, the cell suspension was then added to a conical 15 mL tube, centrifuged at 400 G for 5 min, washed with serum-free medium Dulbecco's Modified Eagle's Medium/Nutrient Mixture F-12 Ham (Cat. No. D6434−500 ML, Sigma-Aldrich, MO, USA), and centrifuged again at 400 G for 5 min. For a total of 1.05×10^6 cells, a stock solution was prepared by adding 1 μL of PKH67 dye to 4.7 μL of ethanol. From this stock solution, 1 μL was then added to 250 μL of diluent C and added to the cells. Cells were incubated with the staining solution for 5 min while mixing periodically with a pipet. After 5 min, the staining process was stopped by adding 250 μL of 1% Bovine Serum Albumin (Cat. No. A2153−10G, Sigma-Aldrich, MO, USA), and this mixture was incubated for 1 min. The cell suspension was then centrifuged at 400 G for 10 min, the supernatant was then discarded, and a complete neuronal progenitor growth medium was added. Cells were then seeded at a cell density of 70,000 cells/well in a 12-well culture plate with the previously coated ES PCL scaffolds and three wells that were used as controls without scaffolds. After 48 h, undifferentiated NPCs were fixed using 4% paraformaldehyde (PFA) for 20 min. Samples were then washed three times with 1X PBS, and DAPI (Thermo Fisher Scientific, Waltham, MA) was used to stain the cell nuclei. Images were acquired using a fluorescent microscope ZEISS AXIO Observer (Zeiss, Germany), and ImageJ Software was used to measure the length of cellular extensions before the differentiation process by taking five measurements from three different images from each condition. The length of cellular extensions was measured using the following formula:

$$\textit{Average Length of Cell Extensions} = (\textit{Sum of Measurements for Total Length of Cell Extensions})/(\textit{Number of Measurements}) \quad (4)$$

After acquiring fluorescent images, the fixed samples were subjected to scanning electron microscopy (SEM) to examine the initial cell morphology of undifferentiated cells within the electrospun scaffolds and their coatings, including CBM, Matrigel, Stock Fibrin (20 mg/mL), and Diluted Fibrin (10 mg/mL). Prior to SEM analysis, the samples underwent sputter-coating with gold/palladium for 3 min using a sputter coater (Gatan Model 682 Precision Etching Coating System Pleasantown, CA, USA), and SEM was conducted using an SEM (SU3500, Hitachi, Japan) at a 10 kV voltage and a current of 101.2 μA at varying magnifications.

2.5.2. Immunostaining and SEM for Confirmation of Cell Differentiation. Immunostaining studies were performed to detect the expression of Tyrosine Hydroxylase (Cat. No. ab137869, Abcam, UK) in differentiated DA neurons. The differentiated DA neurons seeded in the electrospun PCL scaffolds and in 2D controls were washed with 1X PBS three times and fixed with 4% paraformaldehyde (PFA) solution for 15 min at room temperature; samples were then rinsed three times and immersed in 1X PBS and placed on a Belly Dancer shaker at 10 rpm for 5 min. Cells were blocked with a blocking solution (1X PBS, 5% BSA, 0.3% 100X Triton) overnight at 4 °C. After removal of the blocking solution, samples were washed with 1X PBS three times and placed on a Belly Dancer shaker at 10 rpm for 5 min. The primary antibody, Tyrosine Hydroxylase (Cat. No. ab137869, Abcam, UK), was then added to the samples and incubated overnight at 4 °C. The

https://doi.org/10.1021/acsomega.4c03952
ACS Omega 2024, 9, 37063−37075

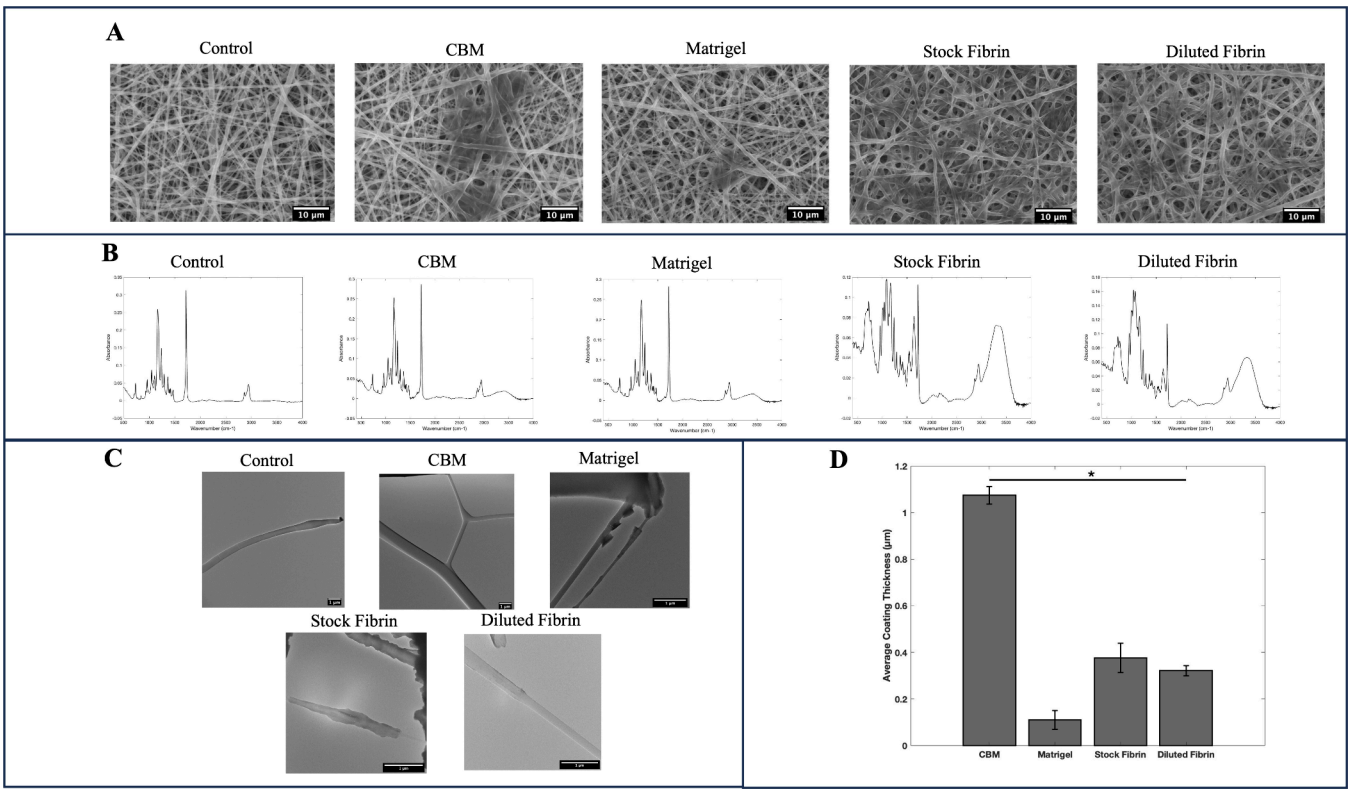

Figure 1. (A) Scanning Electron Microscopy (SEM) Images. (B) ATR-FTIR Results. (C) Transmission Electron Microscopy (TEM) Images. (D) Quantitative analysis of coating thickness of electrospun PCL scaffolds coated with CBM, Matrigel, Stock Fibrin (20 mg/mL), and Diluted Fibrin (10 mg/mL).

samples were then washed three times with 1X PBS. Next, the secondary antibody, Goat Anti-Rabbit Alexa Fluor 488 (Cat. No. ab150077, Abcam, UK), was added and the samples were incubated for 1 h. The secondary antibody solution was removed, and all samples were washed with 1X PBS thrice. Images were acquired using a fluorescence microscope ZEISS AXIO Observer (Zeiss, Germany). Fluorescent images were acquired using a fluorescent microscope ZEISS AXIO Observer (Zeiss, Germany), and ImageJ Software was used to measure the length of cellular extensions in differentiated cells by taking five measurements from three different images from each coating condition. Length of cellular extensions was measured using Equation 4.

After conducting immunostaining studies, the samples were utilized for scanning electron microscopy (SEM) analysis to examine the cell morphology after differentiation of cells seeded in the electrospun scaffolds and their coatings, including CBM, Matrigel, Stock Fibrin (20 mg/mL), and Diluted Fibrin (10 mg/mL). To prepare for SEM analysis, the samples were sputter-coated with gold/palladium for 3 min in a sputter coater (Gatan Model 682 Precision Etching Coating System Pleasantown, CA, USA) and were visualized using SEM (SU3500, Hitachi, Japan) at 10 kV voltage and current of 101.2 μA at varying magnifications.

2.6. Electrophysiological Characterization. Electrophysiological recordings of differentiated cells were acquired using the Axion Maestro Edge multiwell microelectrode array (MEA) and Impedance System (AXION Biosystems, GA, USA). This technology enables the precise recording of extracellular field potentials originating from excitable cells, such as neurons and cardiac cells. By capturing these signals, the system facilitates the measurement of crucial parameters including the number of spikes and firing rates of cells, which were reported in this study. An Axion's MEA plate was prepared by adding 50 μL of 0.1% PEI solution to each well, the plate was left in the incubator at 37 °C, 5% CO_2 for at least 60 min; the PEI solution was then rinsed from the well surface using 200 μL of sterile DI water four times and left overnight to air-dry. After differentiating the cells, cells were passaged following the vendor's instructions and seeded in the MEA plate at a cell density of 20,000 cells/cm^2. After 2 days, daily electrophysiological recordings were acquired. Results comparing firing activity from day 2 and day 6 are reported in this study. This approach has been performed to measure electrophysiological activity in multiple ex-vivo experiments involving mice brain slices;[22,23] thus, this process was implemented to confirm the firing activity from the differentiated DA neurons.

2.7. Statistical Analysis. All experiments were performed in triplicate, and numerical data are reported as mean ± standard deviation. All data were compared using ANOVA and t test with $p < 0.05$ considered to be statistically significant.

3. RESULTS

3.1. Characterization of Uncoated and Coated ES-PCL Scaffolds. ES PCL scaffolds coated (with CBM, Matrigel, Stock Fibrin (20 mg/mL), and Diluted Fibrin (10 mg/mL), uncoated, and acellular were characterized by using SEM, FTIR-ATR, and TEM. Results can be observed in Figure 1. The SEM micrographs acquired for control (uncoated PCL scaffolds) and coated samples are shown in Figure 1A. These micrographs were used to observe the morphology of ES PCL

https://doi.org/10.1021/acsomega.4c03952
ACS Omega 2024, 9, 37063−37075

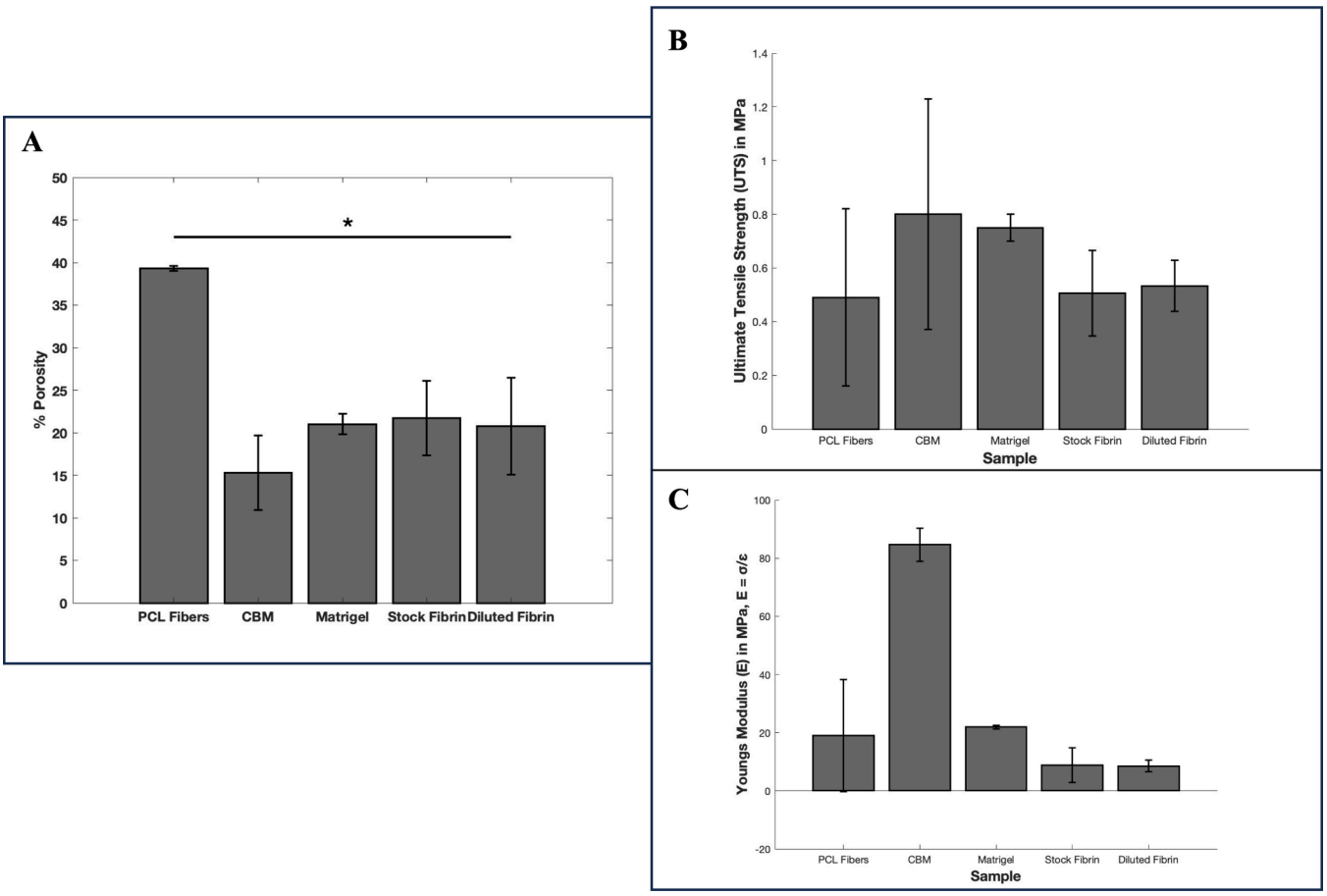

Figure 2. (A) Percentage porosity for PCL Fibers Only (Control), CBM, Matrigel, Stock Fibrin (20 mg/mL), and Diluted Fibrin (10 mg/mL). (B) Ultimate Tensile Strength (UTS) values for PCL Fibers Only (Control), CBM, Matrigel, Stock Fibrin (20 mg/mL), and Diluted Fibrin (10 mg/mL). (C) Young's Modulus (E) values obtained for PCL Fibers Only (Control), CBM, Matrigel, Stock Fibrin (20 mg/mL), and Diluted Fibrin (10 mg/mL).

scaffolds with various coatings as well as quantify the percentage of porosity for each condition. Figure 1A confirms that all scaffolds were coated with various biomaterials, adopted in this study in comparison with uncoated controls.

ATR-FTIR revealed characteristic peaks consistent with PCL indicating its presence within our samples, as observed in Figure 1B. Figure 1B and Supporting Information Figure S2 illustrate the precise identification of individual peaks for each sample. The most eminent peaks that were identified included a peak at ∼3000 cm^{-1} that confirmed the C−H stretching.[24] Another peak was observed at ∼1720 cm^{-1}, which corresponds to C═O stretching bands as well as prominent peaks were observed at ∼1170 to 1240 cm^{-1}, attributed to the C−O−C stretching vibrations arising from the ester groups within PCL.[24]

The presence of CBM coating in ES PCL scaffolds was confirmed by identifying the presence of collagen IV, which is one of the main components of all basement membranes.[25] Results exhibited characteristic peaks that were observed at ∼1025 to 1080 cm^{-1}, which are associated with the C−O and C−O−C absorption bands of carbohydrate moieties.[26] Smaller peaks were observed at ∼1350 and ∼1400 cm^{-1}, which are attributed to the CH_2 and CH_3 absorption bands of collagens.[26] All these peaks confirmed the successful coating of our ES PCL scaffolds.

Furthermore, the results from the PCL-Matrigel coating exhibited characteristic peaks indicative of the presence of Matrigel on the surface of the ES PCL scaffolds. Additional peaks were observed at ∼1240 cm^{-1}, which corresponds to C−O−C stretching and at ∼3000 cm^{-1}, which corresponds to CH_2 stretching vibrations.[27]

In addition, FTIR results from stock fibrin (20 mg/mL) and diluted fibrin (10 mg/mL) coatings indicated the deposition of fibrin in the ES PCL scaffold by observing a broad and stretched characteristic peak at ∼3300 cm^{-1}, which corresponds to the shift of the OH stretching band, caused by the prevalence of N−H stretching absorption bands over the hydroxyl group.[28,29] Likewise, a prominent peak was observed at ∼1640 cm^{-1} and a smaller peak was identified at ∼1540 cm^{-1} which correspond to Amide I and Amide II, respectively.[28,29]

TEM micrographs shown in Figure 1C were used to measure the fiber thickness in uncoated (PCL) samples as well as measure coating thickness (Figure 1D) in coated samples (CBM, Matrigel, Stock Fibrin (20 mg/mL), and Diluted Fibrin (10 mg/mL)) by using eq 1. In uncoated samples, we obtained an average fiber thickness of 0.42 ± 0.06 μm. For CBM coating we obtained an average coating thickness of 1.07 ± 0.37 μm; Matrigel resulted in a coating thickness of 0.11 ± 0.04 μm, Stock Fibrin resulted in a coating thickness of 0.376 ± 0.06 μm, and Diluted Fibrin resulted in a coating thickness of 0.21

https://doi.org/10.1021/acsomega.4c03952
ACS Omega 2024, 9, 37063−37075

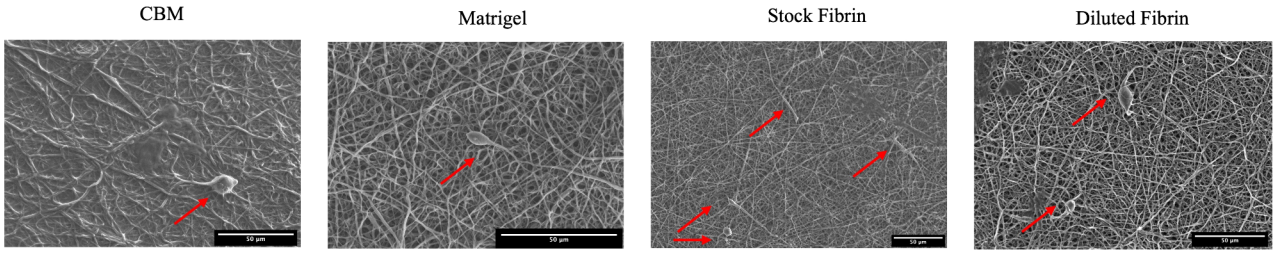

Figure 3. Scanning Electron Microscopy (SEM) Images of Undifferentiated NPCs.

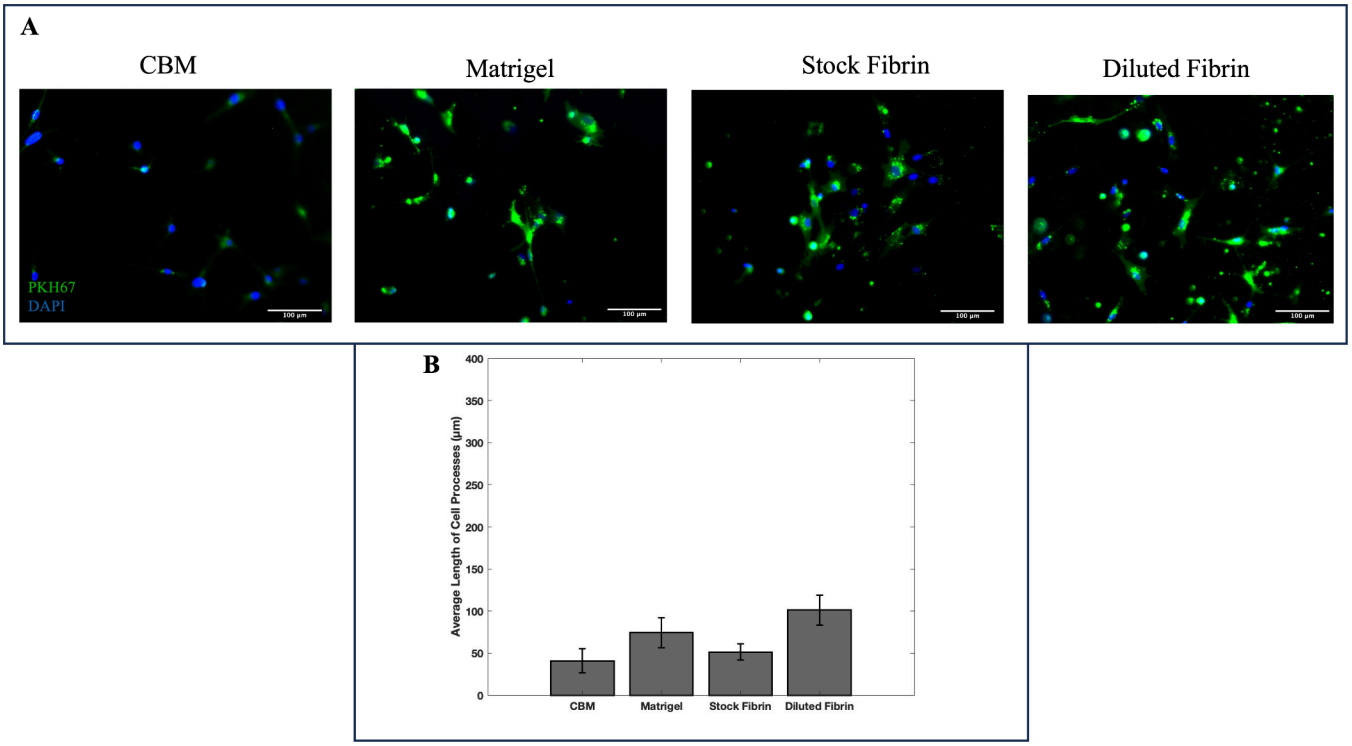

Figure 4. (A) Fluorescence microscopy images of undifferentiated NPCs using DAPI and PKH67. (B) Quantitative analysis of average length of cell processes for undifferentiated NPCs.

± 0.22 μm. The CBM coating was significantly thicker ($p < 0.05$) compared to the other cases. On the contrary, Matrigel coating was significantly thinner compared to all other coatings ($p < 0.05$). The fibrin coatings appeared to be within this range, and the diluted fibrin coating appeared to be more homogeneous and consistent compared to the stock fibrin.

As can be observed in Figure 2A, the extent of porosity was higher in uncoated PCL scaffolds with an average percentage of 39.3 ± 0.31%. Stock fibrin (20 mg/mL), Diluted Fibrin (10 mg/mL), Matrigel, and CBM had an average porosity of 21.7 ± 4.4%, 20.7 ± 5.7%, 21 ± 1.2%, and 15.3 ± 4.4%, respectively. While all coatings significantly reduced sample porosity, the CBM coating reduced it to the maximum extent. The reduction in porosities was statistically significant in all coated scaffolds compared to uncoated samples ($p < 0.05$).

Figures 2B and 2C show the ultimate tensile strength (UTS) and Young's modulus values obtained for all samples during DMA tests. Uncoated samples exhibited an UTS of 0.49 MPa and a Young's modulus of 19 MPa, indicating good mechanical properties. These findings align with ranges reported in existing literature for other viscoelastic biomaterials.[30] Additionally, the mechanical properties of the ES scaffolds were significantly enhanced by the addition of coatings. CBM-coated samples exhibited a UTS of 0.80 MPa and a Young's modulus of 85 MPa. Samples coated with Matrigel showed a UTS of 0.75 MPa and a Young's modulus of 22 MPa. Both Stock Fibrin and Diluted Fibrin coatings also improved the UTS values to 0.51 and 0.53 MPa, respectively, with corresponding Young's modulus values of 8.85 and 8.51 MPa. The mechanical properties of scaffolds are essential for supporting cell viability and influencing cell behavior in tissue engineering applications. Specifically, they affect cell adhesion, migration, and differentiation, ultimately impacting tissue regeneration outcomes.[31]

3.2. Confirmation of Cell Adhesion and Maintenance of Their Undifferentiated State Atop the Scaffolds. SEM was employed to thoroughly investigate both the morphology and behavior of cells in combination with the ES PCL scaffolds utilized for this study. Results indicate successful cell adhesion to the scaffold's surface with all coatings used for this study, which included CBM, Matrigel, Stock Fibrin (20 mg/mL), and Diluted Fibrin (10 mg/mL), as can be observed in Figure 3.

In addition to observing the cell morphology and cell behavior with the scaffold using SEM, we additionally investigated the length of cellular extensions by prestaining the cells before seeding them in the ES PCL scaffolds as

https://doi.org/10.1021/acsomega.4c03952
ACS Omega 2024, 9, 37063−37075

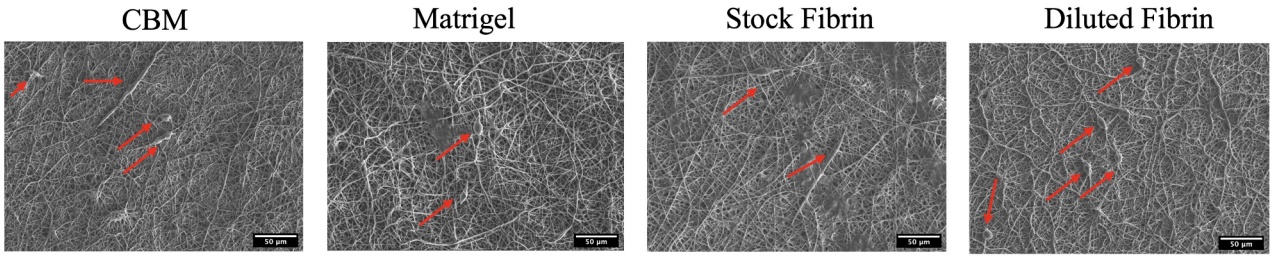

Figure 5. Scanning electron microscopy (SEM) images of differentiated NPCs.

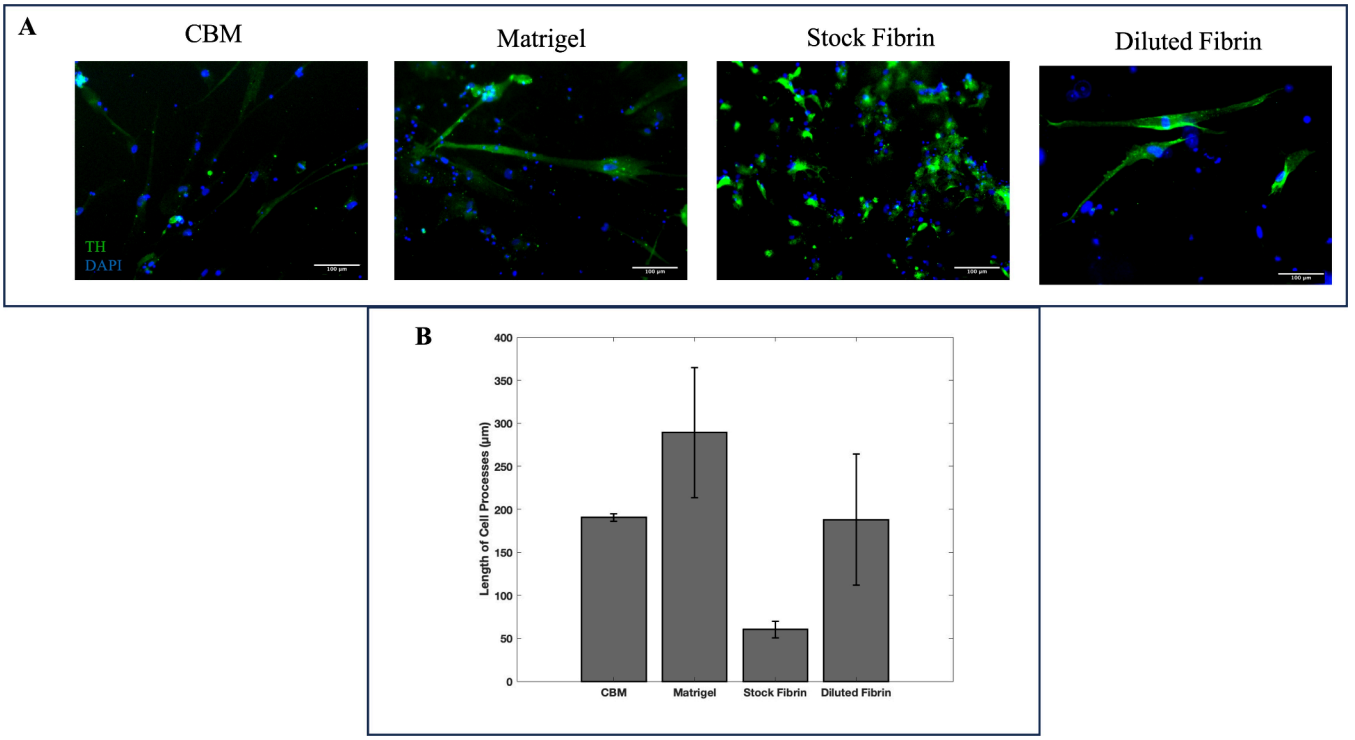

Figure 6. (A) Immunocytochemistry images of differentiated NPCs into dopaminergic (DA) neurons. (B) Quantitative analysis of average length of cell processes in differentiated NPCs.

previously mentioned. Figure 4A shows characteristic images captured from the coated ES scaffolds with the cellular extensions stained green (PKH67) and the cell nuclei stained blue (DAPI). The average length of cellular extensions for all coatings was quantified and depicted in Figure 4B. Undifferentiated NPCs seeded atop CBM coating yielded an average cellular extension length of 40.73 ± 14.21 μm. Cells seeded using Matrigel and Stock Fibrin coatings exhibited an average of 74.2 ± 17.6 μm and 51.3 ± 9.67 μm, respectively. Cells seeded atop Diluted Fibrin exhibited the longest cellular extensions by yielding an average of 101.08 ± 31.9 μm. As can be observed, there was a significantly higher number of cells retained atop the samples that were coated using diluted fibrin followed by stock fibrin in comparison to Matrigel and CBM. To confirm these trends, cells detached from the scaffolds were quantified as previously described. The results showed a significantly higher number of cells retained on samples coated with diluted fibrin (~50,000 cells per scaffold; $p < 0.05$), followed by those coated with stock fibrin (~46,786 cells per scaffold, $p < 0.05$) and Matrigel (~48,000 cells per scaffold, $p < 0.05$), in comparison with CBM (~30,000 cells per scaffold).

3.3. Confirmation of Cell Differentiation and Retention Atop the Scaffolds. After differentiating the cells, SEM was utilized to observe any morphological cellular changes as well as examine cell behavior with the scaffold and coatings used for this study. As can be observed in Figure 5, cells show more elongated cellular extensions in all coatings especially fibrin (stock and diluted) and Matrigel.

The characteristic morphological cellular changes that occur with neuronal differentiation were confirmed by microscopic fluorescent imaging via immunostaining. Figure 6A shows images from immunostaining studies acquired for all coatings with cellular extensions stained in green (TH) and cell nuclei stained in blue (DAPI). Figure 6B shows the quantified results regarding average cellular extensions for all samples. Cells seeded atop CBM coatings yielded an average of cellular extensions of 190 ± 4 μm, whereas cells that were seeded with Matrigel resulted in an average of 289 ± 76 μm. On the other hand, stock fibrin yielded the lowest average of cellular extensions, which resulted in an average of 60 ± 9.5 μm. Lastly, diluted fibrin exhibited an average cell extension of 188 ± 76 μm. In addition, the detection of multipolar cells with laterally and ventrally projecting dendrites confirmed the differentiation of DA neurons and their maturation.[32]

To validate the successful differentiation of NPCs into DA neurons, comprehensive optical examinations were performed

https://doi.org/10.1021/acsomega.4c03952
ACS Omega 2024, 9, 37063−37075

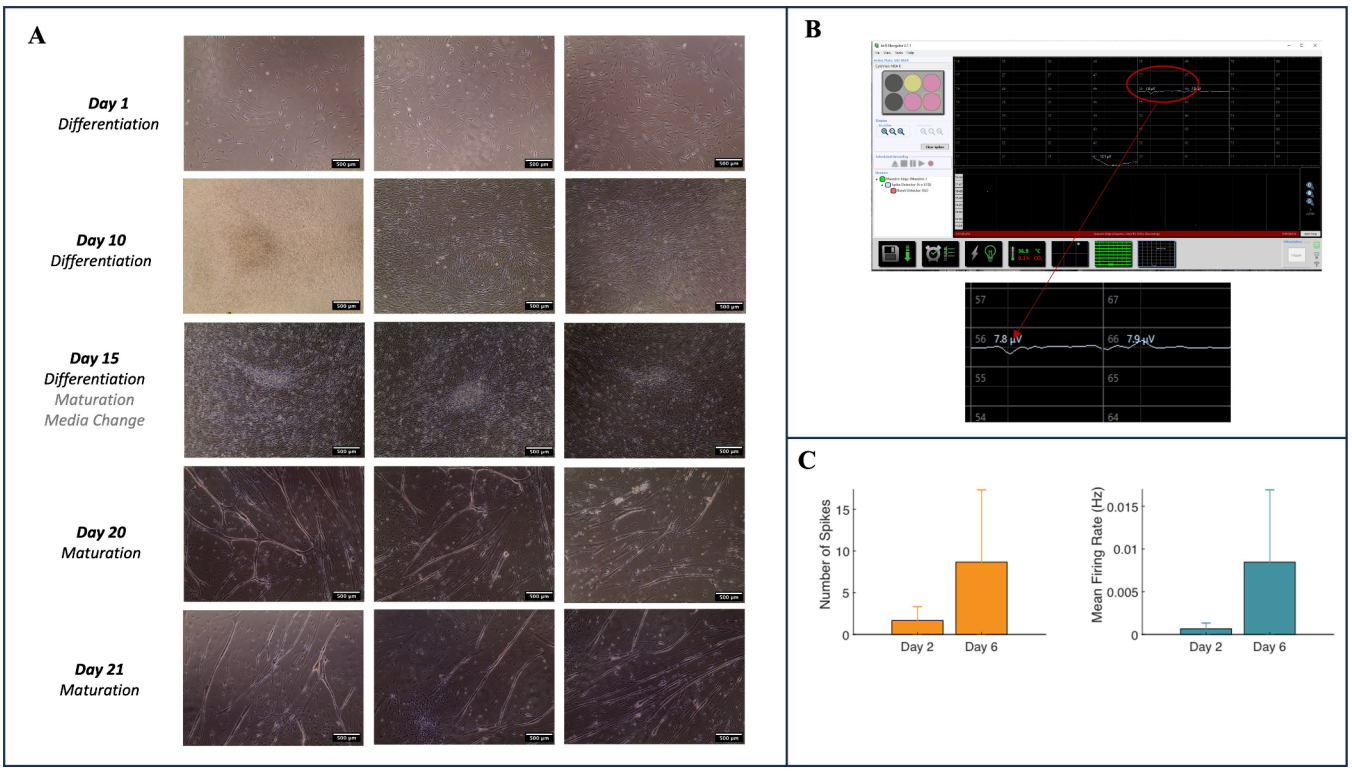

Figure 7. (A) Micrographs of cells during differentiation and maturation, images acquired with EVOS XL Core at 10X magnification. (B) AXION MEA firing spikes data acquisition (Post Day 21). (C) Quantification of number of spikes and mean firing rate for Day 2 and Day 6.

daily throughout the differentiation process. Figure 7A illustrates a notable transformation: initially, at day 1 cells appear spherical; however, as the process unfolds, cellular extensions emerge, which is particularly evident after day 15. This morphological evolution signifies the progression toward mature dopaminergic neuron morphology. Additionally, confirmation of dopaminergic neuron differentiation was validated by conducting electrophysiological studies to assess the firing activity of differentiated cells. Figure 7B shows the firing activity, showcasing evident action potentials as early as day 2 after passaging and seeding the cells. This electrophysiological evidence further supports the successful differentiation process. Figure 7C depicts the quantitative analysis of firing activity. Notably, after 1 week, the Axion Maestro Edge MEA plate with differentiated DA neurons recorded an average of 10 spikes with a mean firing rate of 0.42 Hz. These results are in agreement with other published findings[33] and confirm the successful differentiation and maturation of NPCs into DA neurons.

4. DISCUSSION

The progressive nature of Parkinson's disease poses significant challenges in both treatment and management, compounded by the critical importance of early diagnosis for effective intervention. Existing therapeutic strategies often fall short in providing patients with a satisfactory quality of life, underscoring the pressing need to further explore the disease's pathogenesis and novel treatment modalities. Each year, approximately 50,000 to 60,000 cases are diagnosed in the United States with a prevalence exceeding one million individuals. This disease impacts about 1−2% of the population who are over 65 years old. The prevalence is anticipated to double in the next 20 years.[34] The symptoms of PD primarily stem from the progressive deterioration of dopaminergic (DA) neurons in the substantia nigra, a critical region of the brain involved in movement control.[1] The loss of these neurons leads to a significant decrease in dopamine levels, which is essential for regulating motor function. This neuronal death and dopamine deficiency manifest in the characteristic symptoms of PD, such as tremors, rigidity, bradykinesia, and postural instability.[35]

Several pathological mechanisms contribute to the degeneration of DA neurons in PD, including alpha-synuclein aggregation, mitochondrial dysfunction, and oxidative stress.[36] Alpha-synuclein is a protein that normally plays a role in synaptic function and neurotransmitter release. In PD, alpha-synuclein misfolds and aggregates into insoluble fibrils, forming Lewy bodies within neurons.[36] These aggregates disrupt cellular homeostasis, impair synaptic function, and trigger neuroinflammatory responses, contributing to neuronal death. Likewise, mitochondrial dysfunction is another critical factor in PD pathogenesis. Mitochondria are responsible for producing cellular energy through oxidative phosphorylation.[37] In PD, mitochondrial defects lead to impaired energy production, increased production of reactive oxygen species (ROS), and activation of apoptotic pathways.[38] The resulting energy deficit and oxidative damage further increase neuronal vulnerability and death. Additionally, oxidative stress, characterized by an imbalance between ROS production and antioxidant defenses, plays a significant role in PD. The high metabolic activity of DA neurons makes them particularly susceptible to oxidative damage. Excessive ROS can damage cellular components, including lipids, proteins, and DNA, leading to impaired cellular function and triggering neurodegenerative processes.[39]

The burden of Parkinson's disease, with its increasing prevalence and lack of definitive cure, underscores the urgency

https://doi.org/10.1021/acsomega.4c03952
ACS Omega 2024, 9, 37063−37075

for innovative approaches to neuronal regeneration. Current treatments for PD, such as levodopa, dopamine agonists, MAO-B inhibitors, and deep brain stimulation, provide symptomatic relief but have significant limitations.[40] Levodopa, the most commonly used treatment, is effective in alleviating motor symptoms but often leads to long-term complications like motor fluctuations and dyskinesias. Dopamine agonists and MAO-B inhibitors also help manage symptoms but can cause side effects such as impulsive behaviors and cardiovascular issues. Deep brain stimulation, a surgical option, offers benefits for advanced PD but is invasive and not suitable for all patients. These treatments do not stop the progression of the disease or address the underlying neuronal degeneration, highlighting the need for innovative research approaches.

Tissue engineering emerges as a promising avenue for addressing these complexities. By implementing innovative approaches, such as the creation of disease models using engineered tissues in vitro, tissue engineering offers a platform to explore the underlying mechanisms of Parkinson's disease progression.[34] Through the recreation of microenvironments that mimic the physiological conditions of the nervous system, researchers can gain insights into disease pathology and test the efficacy of potential interventions. To achieve this, ES scaffolds can be implemented to produce nanometer or micrometer-diameter fibers via the electrospinning technique. These scaffolds offer a compelling platform for tissue engineering, especially in neuronal differentiation given their nanofibrous architecture which mimics the natural ECM of neural tissues,[7] as well as providing contact guidance for axons,[41] and supporting cell adhesion and proliferation. Therefore, the integration of ES scaffolds in tissue engineering stands as a promising avenue for enhancing neuronal differentiation and, ultimately, creating efficient therapies for neurological disorders.

PCL was chosen for this study as the material for ES scaffolds due to several key properties including its high biocompatibility and biodegradability, which ensure that this material can be safely integrated into biological systems without eliciting adverse immune responses. This is crucial for scaffolds since they are intended to support cell growth and tissue regeneration. Additionally, PCL has an elastic modulus that allows it to provide mechanical support for cellular interaction,[42] which is essential for maintaining the structural integrity of the scaffold while cells attach, proliferate, and differentiate. Therefore, PCL has been widely utilized by published works.[27,43−45] These properties combined enable it to not only seamlessly integrate with biological systems but also offer essential mechanical support crucial for promoting optimal cell interaction. However, a drawback of ES scaffolds made from synthetic materials like PCL is their limited cell attraction because of their low hydrophilicity;[43] therefore, it is necessary to pair it with materials that are hydrophilic to make it suitable for this application. Thus, this research aimed to utilize ES PCL scaffolds coated with various ECM-based biomaterials, which include Cell Basement Membrane (CBM), Matrigel, Stock Fibrin (20 mg/mL), and Diluted Fibrin (10 mg/mL), and evaluate their suitability for supporting neural progenitor cell (NPC) adhesion, maintenance, and induced differentiation into dopaminergic (DA) neurons.

However, there are no reports utilizing PCL-coated scaffolds with these biomaterials for neuronal differentiation. Instead, previous studies have focused on investigating cellular behavior using the coatings alone[46−49] or by implementing natural polymers such as gelatin in their blended solution for the electrospinning process.[43] In this study, ES PCL scaffolds coated with CBM, Matrigel, and Fibrin were found to be an efficient technique to enhance neuronal differentiation of DA neurons. Incorporating these coatings enhances dendrite formation and cell adhesion; likewise, the architecture of ES scaffolds provides the porosity required to create neuronal networks.

SEM imaging results revealed morphological changes indicative of neuronal differentiation, with cells exhibiting more elongated cellular extensions, particularly in fibrin and Matrigel-coated scaffolds. In comparison to other's published work,[50] cell extensions appear more elongated at 20 days postdifferentiation in our cells seeded on ES PCL-coated scaffolds. Additionally, immunostaining studies further confirmed successful differentiation into DA neurons, with cells seeded atop Matrigel and Diluted Fibrin coatings exhibiting the longest cellular extensions, suggesting a favorable microenvironment for neuronal differentiation. Biochemically, fibrin contains several binding sites for integrins and other cell surface receptors, facilitating signal transduction pathways that promote cellular survival, growth, and differentiation.[51] Thus, our results align with previous studies that have demonstrated fibrin's role in supporting neuronal differentiation.[17,47,52,53] Moreover, both Matrigel and Diluted Fibrin showed higher expression of TH. Fibrin, in particular, can bind and release growth factors such as nerve growth factor (NGF) and brain-derived neurotrophic factor (BDNF), which are essential for TH expression.[54−56] This ability to interact with growth factors likely explains the observed increase in TH expression.

On the other hand, Matrigel is rich in collagen and therefore exerts beneficial effects on NPC culture in this study. Compared to findings in published works,[57,58] the cells exhibited morphological characteristics consistent with differentiated DA neurons. However, observing neuronal networks may be challenging due to the scaffold's fibrous structure. Furthermore, electrophysiological studies provided further validation of successful differentiation into DA neurons. The emergence of cellular extensions over time and the presence of action potentials indicated the progression toward mature dopaminergic neuron morphology, confirming the effectiveness of the differentiation protocol.

This study holds significant importance in the field of biomedical engineering, addressing a crucial need for effective strategies in neural tissue engineering, particularly concerning conditions like Parkinson's disease, where the loss of dopaminergic neurons results in deterioration of motor skills. The research's innovative approach involves comprehensively evaluating various biomaterial coatings on electrospun (ES) polycaprolactone (PCL) scaffolds, shedding light on their efficacy in enhancing cell attachment, differentiation, and the retention of dopaminergic characteristics. The development of a tissue-on-a-chip platform using human induced pluripotent stem cell (hiPSC)-derived neural progenitor cells (NPCs) cultured on these biomaterial-coated scaffolds presents a sophisticated model for studying the early onset and progression of PD. This model not only facilitates a comprehensive investigation into dopaminergic (DA) neuron differentiation and maturation but also provides a platform for testing potential therapeutic interventions in a controlled environment. Moreover, the study's findings demonstrate the efficacy of fibrin-coated scaffolds, particularly those with diluted fibrin, in promoting the differentiation and maturation

https://doi.org/10.1021/acsomega.4c03952
ACS Omega 2024, 9, 37063−37075

of NPCs into dopaminergic neurons. This suggests a promising strategy for neural regeneration, with implications for developing regenerative therapies aimed at replacing damaged neurons in PD patients. By bridging the gap between biomaterial science and neural regeneration, this research has the potential to transform biomedical engineering and open new avenues for treating neurological diseases.

5. CONCLUSION

In conclusion, our study comprehensively assessed the efficacy of various coatings on ES PCL scaffolds for tissue engineering applications, particularly in the context of neuronal stem cell culture and differentiation. The innovative use of PCL-coated scaffolds combined with specific biomaterials to enhance neuronal differentiation is a unique aspect of this study. Unlike previous studies that have focused either on coatings alone or on incorporating natural polymers like gelatin into electrospinning solutions, this research uniquely integrates these biomaterials with PCL-coated scaffolds. This novel approach offers new insights and potential advancements in neural tissue engineering.

Through meticulous characterization utilizing SEM, FTIR, and TEM, we elucidated the morphological and structural changes induced by different coatings. Notably, the coating thickness and porosity of the scaffolds were significantly influenced by the choice of coating material. Furthermore, fluorescent images from prestaining studies and SEM imaging confirmed successful cell adhesion across all coated scaffolds, with Diluted Fibrin and Matrigel coatings particularly enhancing cellular extension lengths, indicating favorable conditions for cell growth and proliferation. Moreover, an enhanced TH expression was remarkably observed in Matrigel and Diluted Fibrin coatings. SEM micrographs additionally demonstrated an increased number of cells in Diluted Fibrin in comparison to other coatings, and electrophysiological studies validated the active electrical firing activity of DA neurons. The observation of cellular differentiation and retention atop the scaffolds provided crucial insights into the efficacy of the coatings in guiding induced DA differentiation. Particularly noteworthy was the significant enhancement of dopaminergic neuron differentiation observed in the diluted fibrin coating, suggesting their potential utility in neural tissue engineering applications.

■ ASSOCIATED CONTENT

Data Availability Statement

All data generated or analyzed during this study are included in this published article (and its Supporting Information files). The raw data sets for all the figures generated during and/or analyzed during the current study are available from the corresponding author upon reasonable request.

Supporting Information

The Supporting Information is available free of charge at https://pubs.acs.org/doi/10.1021/acsomega.4c03952.

Figure S1. Electrospinning Set Up; Figure S2. FTIR Results for A) PCL Fibers, B) Cell Basement Membrane Coating Atop of PCL Fibers, C) Matrigel Coating Atop of PCL Fibers, D) Stock Fibrin (20 mg/mL) Coating Atop of PCL Fibers, and E) Diluted Fibrin (10 mg/mL) Coating Atop of PCL Fibers (PDF)

■ AUTHOR INFORMATION

Corresponding Author

Binata Joddar − *Inspired Materials and Stem-Cell Based Tissue Engineering Lab (IMSTEL), The University of Texas at El Paso, El Paso, Texas 79968, United States; Department of Metallurgical, Materials and Biomedical Engineering, The University of Texas at El Paso, El Paso, Texas 79968, United States; Border Biomedical Research Center, The University of Texas at El Paso, El Paso, Texas 79968, United States;* orcid.org/0000-0002-9157-3140; Email: bjoddar@utep.edu

Authors

Salma P. Ramirez − *Inspired Materials and Stem-Cell Based Tissue Engineering Lab (IMSTEL), The University of Texas at El Paso, El Paso, Texas 79968, United States; Department of Metallurgical, Materials and Biomedical Engineering, The University of Texas at El Paso, El Paso, Texas 79968, United States*

Ivana Hernandez − *Inspired Materials and Stem-Cell Based Tissue Engineering Lab (IMSTEL), The University of Texas at El Paso, El Paso, Texas 79968, United States; Department of Metallurgical, Materials and Biomedical Engineering, The University of Texas at El Paso, El Paso, Texas 79968, United States*

Zayra N. Dorado − *Inspired Materials and Stem-Cell Based Tissue Engineering Lab (IMSTEL), The University of Texas at El Paso, El Paso, Texas 79968, United States; Department of Metallurgical, Materials and Biomedical Engineering, The University of Texas at El Paso, El Paso, Texas 79968, United States*

Carla D. Loyola − *Inspired Materials and Stem-Cell Based Tissue Engineering Lab (IMSTEL), The University of Texas at El Paso, El Paso, Texas 79968, United States; Department of Metallurgical, Materials and Biomedical Engineering, The University of Texas at El Paso, El Paso, Texas 79968, United States*

David A. Roberson − *Department of Metallurgical, Materials and Biomedical Engineering and Polymer Extrusion Lab, The University of Texas at El Paso, El Paso, Texas 79968, United States*

Complete contact information is available at: https://pubs.acs.org/10.1021/acsomega.4c03952

Author Contributions

SPR and IH conducted the experiments, collected all the data and images, performed the data analysis, as well as wrote and edited the manuscript. ZND prepared the ES PCL scaffolds. CDL helped with the differentiation protocol for NPCs into DA neurons. DAR helped with the mechanical analysis performed as part of this study. BJ planned the study, wrote and edited the manuscript, and all authors have approved the final version for submission.

Notes

The authors declare no competing financial interest.

■ ACKNOWLEDGMENTS

The Joddar laboratory (IMSTEL) acknowledges NSF grants #1828268 and #1927628 and NIH SC1 grant #1SC1HL154511-01. We acknowledge the technical assistance received from UT Austin's Texas Materials Institute for material characterization experiments.

REFERENCES

(1) Ramesh, S.; Arachchige, A. S. P. M. Depletion of dopamine in Parkinson's disease and relevant therapeutic options: A review of the literature. *AIMS neuroscience* **2023**, *10* (3), 200.

(2) Willis, A.; et al. Incidence of Parkinson disease in North America. *npj Parkinsons Disease* **2022**, *8* (1), 170.

(3) Joshi, R.; et al. PKG movement recording system use shows promise in routine clinical care of patients with Parkinson's disease. *Frontiers in neurology* **2019**, *10*, 1027.

(4) Willerth, S. M.; et al. Optimization of fibrin scaffolds for differentiation of murine embryonic stem cells into neural lineage cells. *Biomaterials* **2006**, *27* (36), 5990−6003.

(5) Xu, W.; Lakshman, N.; Morshead, C. M. Building a central nervous system: the neural stem cell lineage revealed. *Neurogenesis* **2017**, *4* (1), No. e1300037.

(6) Martínez-Cerdeño, V.; Noctor, S. C. Neural progenitor cell terminology. *Frontiers in neuroanatomy* **2018**, *12*, 104.

(7) Ahmadi, S.; Shafiei, S. S.; Sabouni, F. Electrospun nanofibrous scaffolds of polycaprolactone/gelatin reinforced with layered double hydroxide nanoclay for nerve tissue engineering applications. *ACS omega* **2022**, *7* (32), 28351−28360.

(8) Paulsson, M. Basement membrane proteins: structure, assembly, and cellular interactions. *Crit. Rev. Biochem. Mol. Biol.* **1992**, *27* (1−2), 93−127.

(9) Salimbeigi, G.; et al. Basement membrane properties and their recapitulation in organ-on-chip applications. *Materials Today Bio* **2022**, *15*, 100301.

(10) Jin, K.; et al. Transplantation of human neural precursor cells in Matrigel scaffolding improves outcome from focal cerebral ischemia after delayed postischemic treatment in rats. *Journal of Cerebral Blood Flow & Metabolism* **2010**, *30* (3), 534−544.

(11) Weisel, J. W.; Litvinov, R. I. Fibrin formation, structure and properties. *Fibrous proteins: structures and mechanisms* **2017**, *82*, 405−456.

(12) Chandrababu, K.; Senan, M.; Krishnan, L. K. Exploitation of fibrin-based signaling niche for deriving progenitors from human adipose-derived mesenchymal stem cells towards potential neural engineering applications. *Sci. Rep.* **2020**, *10* (1), 7116.

(13) Sanz-Horta, R.; et al. Technological advances in fibrin for tissue engineering. *J. Tissue Engineering* **2023**, *14*, 20417314231190288.

(14) Nagiah, N.; et al. Development and Characterization of Furfuryl-Gelatin Electrospun Scaffolds for Cardiac Tissue Engineering. *ACS Omega* **2022**, *7* (16), 13894−13905.

(15) Nagiah, N.; El Khoury, R.; Othman, M. H.; Akimoto, J.; Ito, Y.; Roberson, D. A.; Joddar, B. Development and Characterization of Furfuryl-Gelatin Electrospun Scaffolds for Cardiac Tissue Engineering. *ACS Omega* **2022**, *7* (16), 13894−13905.

(16) dos Santos Bronel, B. A.; et al. Effect of extracellular vesicles derived from induced pluripotent stem cells on mesangial cells underwent a model of fibrosis in vitro. *Sci. Rep.* **2023**, *13* (1), 15749.

(17) Kolehmainen, K.; Willerth, S. M. Preparation of 3D fibrin scaffolds for stem cell culture applications. *JoVE (Journal of Visualized Experiments)* **2012**, No. 61, No. e3641.

(18) Noisa, P.; Raivio, T.; Cui, W. Neural progenitor cells derived from human embryonic stem cells as an origin of dopaminergic neurons. *Stem cells international* **2015**, *2015*, 1.

(19) Tang, Y.; et al. Neural progenitor cells derived from adult bone marrow mesenchymal stem cells promote neuronal regeneration. *Life Sciences* **2012**, *91* (19), 951−958.

(20) Haeri, M.; Haeri, M. ImageJ plugin for analysis of porous scaffolds used in tissue engineering. *Journal of Open Research Software* **2015**, *3* (1), No. e1-e1.

(21) Hernandez, I.; et al. A Semi-Three-Dimensional Bioprinted Neurocardiac System for Tissue Engineering of a Cardiac Autonomic Nervous System Model. *Bioengineering* **2023**, *10* (7), 834.

(22) Dossi, E.; et al. Functional Regeneration of the ex-vivo Reconstructed Mesocorticolimbic Dopaminergic System. *Cerebral Cortex* **2013**, *23* (12), 2905−2922.

(23) Mannal, N., et al., Multi-Electrode Array Analysis Identifies Complex Dopamine Responses and Glucose Sensing Properties of Substantia Nigra Neurons in Mouse Brain Slices. *Frontiers in Synaptic Neuroscience*, **2021**. *13*. DOI: 10.3389/fnsyn.2021.635050

(24) Elzein, T.; et al. FTIR study of polycaprolactone chain organization at interfaces. *J. Colloid Interface Sci.* **2004**, *273* (2), 381−387.

(25) Boudko, S. P.; et al., Basement membrane collagen IV: Isolation of functional domains. In *Methods in cell biology*, Elsevier, 2018; pp 171−185.

(26) Belbachir, K.; et al. Collagen types analysis and differentiation by FTIR spectroscopy. *Anal. Bioanal. Chem.* **2009**, *395*, 829−837.

(27) Ghasemi-Mobarakeh, L.; et al. Bio-functionalized PCL nanofibrous scaffolds for nerve tissue engineering. *Materials Science and Engineering: C* **2010**, *30* (8), 1129−1136.

(28) Pankajakshan, D.; et al. Development of a fibrin composite-coated poly (ε-caprolactone) scaffold for potential vascular tissue engineering applications. *Journal of Biomedical Materials Research* **2008**, *87B* (2), 570−579.

(29) Cavalu, S.; et al. Fibrinogen adsorption onto bioglass aluminosilicates. *Rom. J. Biophys* **2007**, *17* (4), 237−245.

(30) Bertocchi, M. J.; et al. Enhanced mechanical damping in electrospun polymer fibers with liquid cores: applications to sound damping. *ACS Applied Polymer Materials* **2019**, *1* (8), 2068−2076.

(31) Nitti, P.; et al. Cell-tissue interaction: the biomimetic approach to design tissue engineered biomaterials. *Bioengineering* **2023**, *10* (10), 1122.

(32) Grace, A. A.; Onn, S.-P. Morphology and electrophysiological properties of immunocytochemically identified rat dopamine neurons recorded in vitro. *J. Neurosci.* **1989**, *9* (10), 3463−3481.

(33) Paladini, C. A.; et al. Dopamine controls the firing pattern of dopamine neurons via a network feedback mechanism. *Proc. Natl. Acad. Sci. U. S. A.* **2003**, *100* (5), 2866−2871.

(34) Harris, J. P.; et al. Emerging regenerative medicine and tissue engineering strategies for Parkinson's disease. *npj Parkinsons Disease* **2020**, *6* (1), 4.

(35) Váradi, C. Clinical features of Parkinson's disease: the evolution of critical symptoms. *Biology* **2020**, *9* (5), 103.

(36) Risiglione, P.; et al. Alpha-synuclein and mitochondrial dysfunction in Parkinson's disease: the emerging role of VDAC. *Biomolecules* **2021**, *11* (5), 718.

(37) Brand, M.; et al. The role of mitochondrial function and cellular bioenergetics in ageing and disease. *British Journal of Dermatology* **2013**, *169* (s2), 1−8.

(38) Perier, C.; Vila, M. Mitochondrial biology and Parkinson's disease. *Cold Spring Harbor perspectives in medicine* **2012**, *2* (2), a009332.

(39) Guo, C.; et al. Oxidative stress, mitochondrial damage and neurodegenerative diseases. *Neural regeneration research* **2013**, *00* (21), 2003−2014.

(40) Jankovic, J.; Aguilar, L. G. Current approaches to the treatment of Parkinson's disease. *Neuropsychiatric disease and treatment* **2008**, *4* (4), 743−757.

(41) Puhl, D. L.; et al. Electrospun fiber scaffolds for engineering glial cell behavior to promote neural regeneration. *Bioengineering* **2021**, *8* (1), 4.

(42) Janmohammadi, M.; Nourbakhsh, M. Electrospun polycaprolactone scaffolds for tissue engineering: a review. *International Journal of Polymeric Materials and Polymeric Biomaterials* **2019**, *68* (9), 527−539.

(43) Ghasemi-Mobarakeh, L.; et al. Electrospun poly (ε-caprolactone)/gelatin nanofibrous scaffolds for nerve tissue engineering. *Biomaterials* **2008**, *29* (34), 4532−4539.

(44) Gautam, S.; Dinda, A. K.; Mishra, N. C. Fabrication and characterization of PCL/gelatin composite nanofibrous scaffold for tissue engineering applications by electrospinning method. *Materials Science and Engineering: C* **2013**, *33* (3), 1228−1235.

https://doi.org/10.1021/acsomega.4c03952
ACS Omega 2024, 9, 37063−37075

(45) Fu, W.; et al. Electrospun gelatin/PCL and collagen/PLCL scaffolds for vascular tissue engineering. *International journal of nanomedicine* **2014**, 2335−2344.
(46) Navaei-Nigjeh, M.; et al. Enhancing neuronal growth from human endometrial stem cells derived neuron-like cells in three-dimensional fibrin gel for nerve tissue engineering. *J. Biomed. Mater. Res., Part A* **2014**, *102* (8), 2533−2543.
(47) Montgomery, A.; et al. Engineering personalized neural tissue by combining induced pluripotent stem cells with fibrin scaffolds. *Biomaterials Science* **2015**, *3* (2), 401−413.
(48) Lee, S.-W.; et al. Optimization of Matrigel-based culture for expansion of neural stem cells. *Animal Cells and Systems* **2015**, *19* (3), 175−180.
(49) Uemura, M.; et al. Matrigel supports survival and neuronal differentiation of grafted embryonic stem cell-derived neural precursor cells. *Journal of neuroscience research* **2010**, *88* (3), 542−551.
(50) Garcia-Parra, P.; et al. A neural extracellular matrix-based method for in vitro hippocampal neuron culture and dopaminergic differentiation of neural stem cells. *BMC neuroscience* **2013**, *14*, 1−13.
(51) Petersen, M. A.; Ryu, J. K.; Akassoglou, K. Fibrinogen in neurological diseases: mechanisms, imaging and therapeutics. *Nat. Rev. Neurosci.* **2018**, *19* (5), 283−301.
(52) Lu, P.; et al. Long-distance growth and connectivity of neural stem cells after severe spinal cord injury. *Cell* **2012**, *150* (6), 1264−1273.
(53) de la Vega, L.; et al. 3D bioprinting models of neural tissues: The current state of the field and future directions. *Brain Res. Bull.* **2019**, *150*, 240−249.
(54) Strömberg, I.; Humpel, C. Expression of BDNF and trk B mRNAs in comparison to dopamine D1 and D2 receptor mRNAs and tyrosine hydroxylase-immunoreactivity in nigrostriatal in oculo co-grafts. *Developmental brain research* **1995**, *84* (2), 215−224.
(55) Hill, C. E.; Hendry, I. Differences in sensitivity to nerve growth factor of axon formation and tyrosine hydroxylase induction in cultured sympathetic neurons. *Neuroscience* **1976**, *1* (6), 489−IN25.
(56) Miller, F. D.; Mathew, T. C.; Toma, J. G. Regulation of nerve growth factor receptor gene expression by nerve growth factor in the developing peripheral nervous system. *J. Cell Biol.* **1991**, *112* (2), 303−312.
(57) Betarbet, R.; et al. Dopaminergic neurons intrinsic to the primate striatum. *J. Neurosci.* **1997**, *17* (17), 6761−6768.
(58) Cossette, M.; Lecomte, F.; Parent, A. Morphology and distribution of dopaminergic neurons intrinsic to the human striatum. *Journal of chemical neuroanatomy* **2005**, *29* (1), 1−11.

https://doi.org/10.1021/acsomega.4c03952
ACS Omega 2024, 9, 37063−37075